

***Ab initio* calculations of $\text{CaCu}_3\text{Ti}_4\text{O}_{12}$ under high pressure: Structural and electronic properties**

Solange B. Fagan,* A. G. Souza Filho, A. P. Ayala, and J. Mendes Filho

Departamento de Física, Universidade Federal do Ceará, 60455-900 Fortaleza, Ceará, Brazil

(Received 31 March 2004; revised manuscript received 18 April 2005; published 5 July 2005)

We calculate structural and electronic properties of $\text{CaCu}_3\text{Ti}_4\text{O}_{12}$ from ambient pressure up to 10.0 GPa using total-energy first-principles methods. Analysis of the simulated high-pressure structure suggests a pressure-induced structural phase transition between 3 and 4 GPa with the crystalline structure changing from $\text{Im}\bar{3}$ (cubic) to $R\bar{3}$ (rhombohedral). By analyzing the electronic band structure, we have observed a pressure-induced semiconductor-metallic transition between 6 and 7 GPa.

DOI: [10.1103/PhysRevB.72.014106](https://doi.org/10.1103/PhysRevB.72.014106)

PACS number(s): 61.50.-f, 71.15.-m, 71.20.-b, 75.75.+a

I. INTRODUCTION

The complex perovskite $\text{CaCu}_3\text{Ti}_4\text{O}_{12}$ (CCTO) has been the subject of intense investigations owing to its remarkable dielectric properties. It has been reported as having the largest dielectric constant ($\epsilon' \approx 10^5$) ever measured in the laboratory.¹⁻³ In addition, ϵ' is nearly constant over a wide temperature range (from 100 K to 600 K). Many models have been proposed aiming to explain the physical basis of the anomalous dielectric constant. Some authors have attributed the high value to extrinsic factors such as defects and grain boundaries.^{4,5} This is supported by theoretical studies which report that the contribution of lattice effects to the dielectric response is only about 60.^{6,7}

The crystalline structure of CCTO is body-centered cubic with eight ATiO_3 perovskite-type formula units per unit cell (where A is either Ca or Cu). The crystalline structure at room temperature and ambient pressure belongs to the centrosymmetric space group $\text{Im}\bar{3}$. No evidence of structural phase transformation under temperature variation has been observed.⁸ However, a neutron scattering study has indicated a transition from paramagnetic to antiferromagnetic phase at a Néel temperature of $T_N = 24$ K.^{9,10} The ground state properties of CCTO were studied^{6,7} using density functional theory within the local spin-density approximation (LSDA) and considering a plane-wave basis set. These studies confirm the stability of the $\text{Im}\bar{3}$ structure and exclude the possibility of classifying this material as a ferroelectric. Furthermore, they also show that CCTO has a semiconductor behavior with a minimum direct band gap of 0.27 eV. No instabilities of the zone-center phonon modes were observed, confirming the absence of temperature-induced phase transitions.²

Besides some reports on the effects of temperature on the physical properties of CCTO there are very few studies about CCTO under pressure.²³ The knowledge of the CCTO properties at different pressures is of scientific interest since there are not yet theoretical reports on this issue. The external high pressure is not directly a relevant degree of freedom on the devices. However, thin films experiment some stress due to substrate and this certainly affects their physical properties and prevents one from tuning the dielectric properties for a rational use in a given device. Therefore, it is of great interest to know how the CCTO properties change under pressure

for better understanding of the behavior of CCTO thin films. Due to its integrability to current technology, this CCTO-based system is the most promising to be used in electronic devices.

In order to shed further light on the structural and electronic properties of CCTO and to improve the knowledge of its phase diagram, we have studied CCTO under pressure variation using total-energy *ab initio* calculations. We have observed a pressure-induced phase transition from cubic $\text{Im}\bar{3}$ to rhombohedral $R\bar{3}$ structure in the 3–4 GPa pressure range. Furthermore, we have observed a pressure-induced semiconductor-metallic transition between 6 and 7 GPa.

II. METHODOLOGY

In order to investigate electronic and structural properties of CCTO under hydrostatic pressure we performed total-energy *ab initio* calculations, based on spin-polarized density-functional theory.^{11,12} We used the SIESTA code,^{13,14} which performs full self-consistent calculations solving the Kohn-Sham (KS) equations. The KS orbitals are expanded using linear combinations of pseudoatomic orbitals proposed by Sankey and Niklewski.¹⁵ In all calculations we used a double-zeta basis set with polarization functions.^{13,14,16} For the exchange and correlation terms, the LSDA¹⁷ was used. Core electrons were replaced by *ab initio* norm-conserving fully separable Troullier-Martins pseudopotentials.¹⁸ Due to the large overlap between the semicore and the valence states, the $3s$ and $3p$ electrons of Ti were explicitly included in the calculation.¹⁹ A cutoff of 150 Ry for the grid integration was used to represent the charge density. We used a $2 \times 2 \times 2$ Monkhorst-Pack k -point mesh for the Brillouin zone integration which has been shown to represent correctly the properties with a good convergence. The atomic distances are modified less than 1% and the electronic properties of the system do not change when a $3 \times 3 \times 3$ mesh was used.^{6,7} All calculations were performed using a 40-atom cubic cell, although the atomic coordinates and total charge density have the periodicity of a 20-atom primitive cell. The CCTO unit cell and the atomic positions were relaxed, allowing the system to reach the desired pressure value, using a conjugated gradient algorithm, until the residual forces were smaller than $0.05 \text{ eV } \text{Å}^{-1}$ and the stress tensor was within 5%–10%

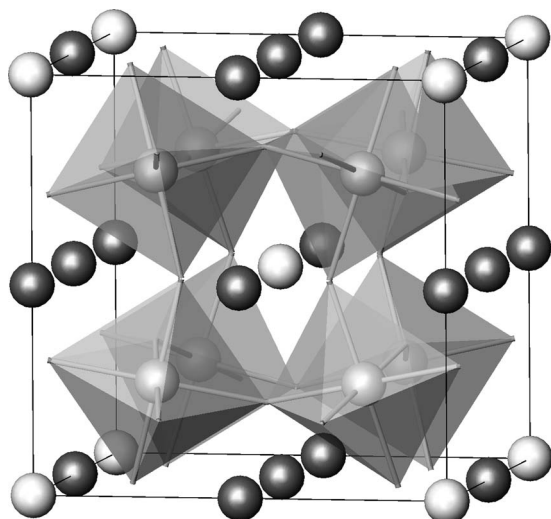


FIG. 1. The $Im\bar{3}$ crystalline structure of $CaCu_3Ti_4O_{12}$. The octahedra represent the TiO_6 groups with O at the corners and Ti at the center. The blank and gray spheres represent Ca and Cu atoms, respectively.

of the value required. It should be pointed out that the minimization of the energy was carried out by using the constant pressure as a constraint. In this case, the system naturally evolves to the state of minimum enthalpy.

III. RESULTS AND DISCUSSION

A. Structural properties

From the theoretical analysis, at $P=0.0$ GPa, the CCTO crystalline structure belongs to the $Im\bar{3}$ cubic body-centered space group (see Fig. 1) and the atomic species Ca, Cu, Ti, and O are placed at $2a, 6b, 8c,$ and $24g$ Wyckoff sites, respectively. Ti cations are sixfold coordinated by equidistant oxygens (Ti-O bond length of 1.964 Å) arranged in slightly distorted TiO_6 octahedra. These octahedra are tilted (Ti-O-Ti bond angle of 140.64°) with respect to the crystallographic axes but their faces are aligned along the $[111]$ diagonal of the cubic lattice. Ca atoms are surrounded by 12 equidistant oxygens (Ca-O bond length of 2.607 Å) whereas all the Cu ions are bounded by a planar arrangement of four oxygen atoms (Cu-O bond length of 1.963 Å). These bond lengths and bond angles values come from theory.

The equilibrium lattice parameter is determined by minimization of the total energy as a function of the supercell volume. In the CCTO structure without pressure ($P=0.0$ GPa) a lattice parameter of 7.398 Å was obtained, which is very close to the experimental value of 7.384 Å measured at low temperatures.⁶ The discrepancy (less than 1%) between theoretical and experimental values for the lattice parameter is associated to the used basis set. In recent LSDA *ab initio* calculations using plane waves as basis set, He *et al.*⁷ obtained a lattice parameter of 7.320 Å.^{20,21}

The structural and electronic properties of CCTO under high pressure were calculated by imposing the constant pressure as a constraint. Specifically, we have calculated the sys-

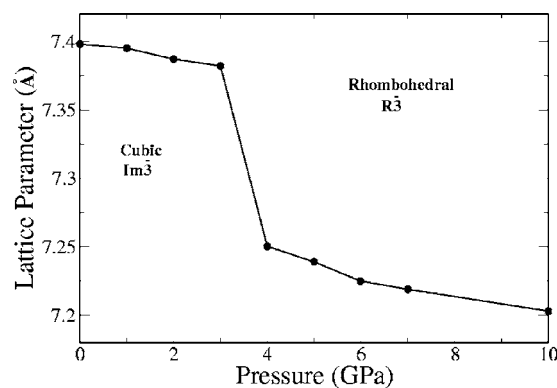


FIG. 2. The lattice parameter Å versus pressure for the CCTO under hydrostatic pressure.

tem at pressures of 0.0, 1.0, 2.0, 3.0, 4.0, 5.0, 6.0, 7.0, and 10.0 GPa. The optimized structure is reached through the minimization of the enthalpy of the system. The calculated lattice parameter versus pressure plot is shown in Fig. 2. It is clear the abrupt change in the lattice parameter between 3 and 4 GPa, thereby indicating that pressure induces a structural phase transition in CCTO. We now discuss this structural transformation from a crystallographic point of view.

The main effect of pressure is to further distort the coordination sphere of the atoms. However, the lattice parameter of the relaxed structure does not exhibit evident departure from a cubic system. The appearing or loss of the symmetry elements is hard to detect by direct inspections of the atomic positions. In order to monitor the CCTO crystalline structures under pressure variation we calculated the structure factor $F(h,k,l)$ for the relaxed supercells obtained from the *ab initio* simulations. The structure factor $F(h,k,l)$ is defined as $F(h,k,l) = \sum_j f(j) \exp[2\pi i(hx_j + ky_j + lz_j)]$, where $f(j)$ is the atomic scattering factor, and $h, k,$ and l stand for Miller indices. The index j runs over all the atoms in the unit cell. The atomic positions $x_j, y_j,$ and z_j are obtained from the *ab initio* simulation after the system reaches its equilibrium for a given pressure. The atomic scattering factors are available for each element in crystallographic databases. In an x-ray or neutron diffraction experiment, the intensity of the diffracted radiation is determined by the structure factor, which contains all the information related to the crystalline structure. We can use the structure factor values for simulating the expected neutron powder diffraction pattern of CCTO. The predicted results ($\lambda=1$ Å) at selected pressures are shown in Fig. 3. In this figure, one can notice that for 0 and 3 GPa the $h+k+l=2n$ (n is an integer number) reflection condition is fulfilled, thus confirming that in this pressure range the CCTO structure is described by a cubic body-centered lattice. Conversely, for pressures higher than 3.0 GPa, this condition is not fulfilled (we can observe the peaks 100 and 210 in Fig. 3) and the structure factor distribution of a primitive lattice is obtained. In order to find the structure of the CCTO phase for $P > 3.0$ GPa, a search for the symmetry operations present in the supercell was carried out using the PLATON package.²² As a result we obtain as the more probable structure a rhombohedral centrosymmetric lattice belonging to the $R\bar{3}$ space group. It should be pointed out that recent high-

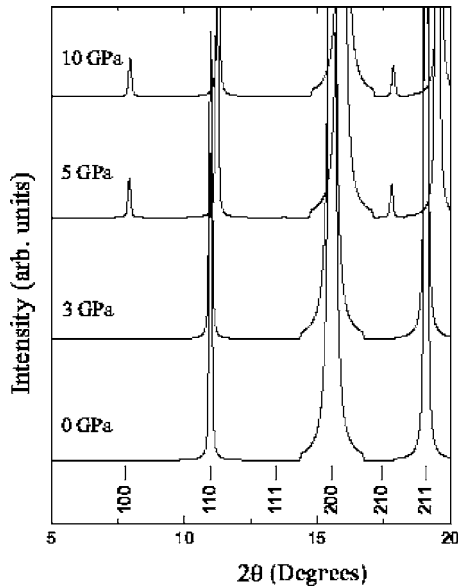


FIG. 3. Calculated neutron powder diffraction patterns ($\lambda = 1 \text{ \AA}$) of CCTO at selected pressures. The h, k, l Miller indices are displayed in the bottom part of the figure.

pressure x-ray studies performed at 300 K have suggested that at room temperature the cubic structure remains stable up to 46 GPa.²³ However, this result does not invalidate our theoretical predictions since our calculations were performed at 0 K. The experiments to be appropriately compared with our predictions should be performed at low temperatures. This result suggest that the rhombohedral structure should be stable only at low temperatures and high pressures.

The parameters of the new crystalline structure are shown in Table I and the arrangement of the TiO_6 oxygen octahedra is drawn in Fig. 4. As can be observed in the $[1\bar{1}\bar{1}]$ projection of the new structure [Fig. 4(a)], the TiO_6 network exhibits a similar arrangement to that of uncompressed CCTO (Fig. 1). However, the oxygen octahedra are no longer aligned along the trigonal axis and a small tilting between consecutive

TABLE I. The calculated atomic positions of $\text{CaCu}_3\text{Ti}_4\text{O}_{12}$ at $P=10.0$ GPa obtained through *ab initio* calculations, where a is the lattice parameter. The calculated a value at this pressure was found to be 7.20 \AA .

Atom	Site	x/a	y/a	z/a
Ca(1)	$\bar{3}$	0	0	0
Ca(2)	$\bar{3}$	0	0	0.5
Cu(1)	$\bar{1}$	0.5	0	0
Cu(2)	$\bar{1}$	0.5	0	0.5
Ti(1)	3	0	0	0.248
Ti(2)	1	0	0.5	0.747
O(1)	1	0.141	0.154	0.161
O(2)	1	0.690	0.196	0.001
O(3)	1	0.4096	0.296	0.291
O(4)	1	0.109	0.403	0.209

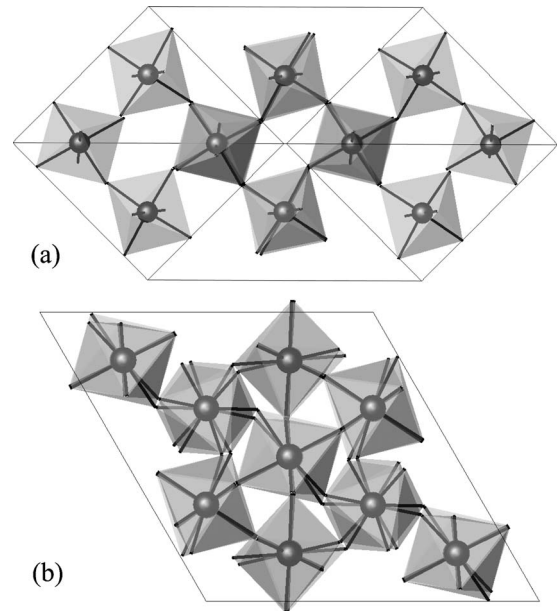


FIG. 4. The (a) $[1\bar{1}\bar{1}]$ projection and (b) $[111]$ projection of the TiO_6 octahedra arrangement for the $\text{CaCu}_3\text{Ti}_4\text{O}_{12}$ structure at $P = 10.0$ GPa. The oxygens are in the vertices of the octahedra.

TiO_6 groups is induced by pressure [see Fig. 4(b)]. As a consequence, a doubling of the unit cell is necessary to describe the periodicity of the new structure, where two nonequivalent sites of each cationic species (Ca, Cu, and Ti) and two of each anionic species (O) give rise to six molecules per unit cell. Note that there are two sets of TiO_6 octahedra, namely (i) Ti(1) linked to O(1) and O(2) and (ii) Ti(2) enclosed by O belonging to all nonequivalent sites at different distances. This atomic distribution induces an extra tilting in the octahedra linked by O(2) [Ti(1)-O(2)-Ti(2) bond angle of 144.3°] while the tilting of the remaining groups is close to the uncompressed value ($\sim 140^\circ$). In the high-pressure phase, each Ca and Cu crystalline site is surrounded by two kinds of oxygen anion. Thus, in the case of Cu cations, which have an important contribution to the electronic band structure and long-range magnetic order, two nonequivalent CuO_4 planar polyhedra are present in the structure. However, the anions of each group are no longer equidistant and they are distributed in two sets of Cu-O bond lengths and angles.

B. Electronic properties

Figure 5 shows the electronic band structure of CCTO at 0.0 GPa. In the absence of applied pressure the CCTO behaves as a semiconductor as can be inferred from its band diagram. We calculate a minimum direct band gap of 0.24 eV at the X high-symmetry point and an indirect band gap of 0.18 eV for the electronic band structure shown in Fig. 5. The indirect band gap is taken as the difference between the valence band maximum at the R high-symmetry point and the conduction band minimum at the X point of the Brillouin zone. Our calculated direct band gap considerably underestimates the experimental value of 1.5 eV.⁶ This electronic band structure discrepancy can be associated with the DFT ap-

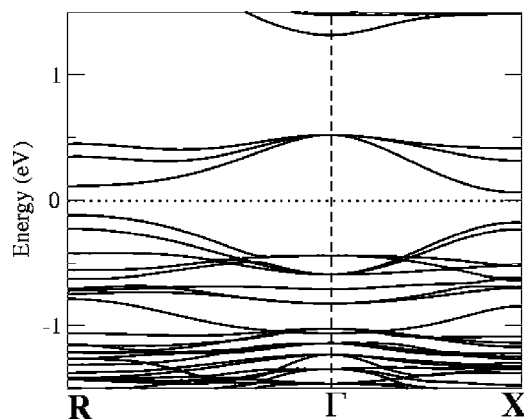


FIG. 5. The electronic band structure of CCTO at $P=0.0$ GPa. The dashed horizontal line corresponds to the Fermi level.

proach. The underestimation of values for the gap has been identified as coming mainly from the $3d$ orbitals localized on the Cu^{2+} ions which result in strong Coulomb interactions that are not adequately treated within LSDA. He *et al.*,⁶ using density-functional theory and LSDA approximation with plane waves as basis set, obtained the values of 0.27 and 0.19 eV for the minimum direct and indirect band gap, respectively. Our results using a different basis set are therefore in good agreement with previous *ab initio* calculations.⁷

The occupied states just below the Fermi energy are found to consist mainly of Cu- $3d$ and O- $2p$ orbitals, being dominated by the Cu- $3d$ orbitals especially in the energy range from -2.0 to -0.5 eV. In the unoccupied conduction band, from Fermi energy (0.0 eV) up to 1.0 eV, the three bands (degenerate at the Γ point) consisting mainly of Cu and O antibonding levels, are observed. Ti- $3d$ orbitals degenerate into t_{2g} and e_g levels and are located, respectively, at about 2.5 and 4.5 eV in the conduction band (not shown in Fig. 5).

Figure 6 shows the total (majority+minority spin states) electronic densities of states (DOS) of CCTO for the uncompressed system [Fig. 6(a)] and with applied pressure of 6.0,

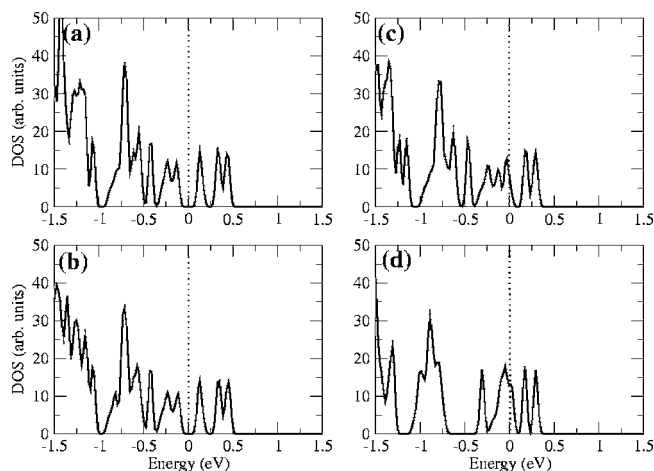


FIG. 6. The electronic densities of states (majority+minority spin states) plots of CCTO for different pressures. (a) $P=0.0$ GPa, (b) $P=6.0$ GPa, (c) $P=7.0$ GPa, and (d) $P=10.0$ GPa. The dotted vertical lines correspond to the Fermi level.

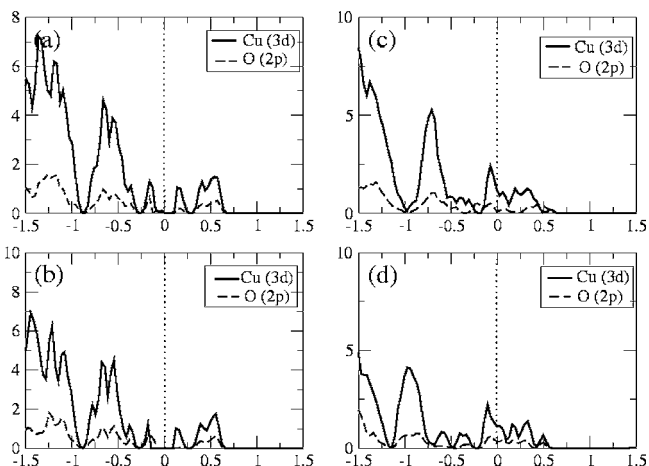


FIG. 7. The projected densities of states (majority+minority spin states) plots of CCTO for Cu- $3d$ (solid lines) and O- $2p$ (dashed lines) orbitals at different pressures. (a) $P=0.0$ GPa, (b) $P=6.0$ GPa, (c) $P=7.0$ GPa, and (d) $P=10.0$ GPa. The dotted vertical lines correspond to the Fermi level.

7.0, and 10.0 GPa [Figs. 6(b)–6(d), respectively]. We can observe from the DOS profiles that up to the pressure of 6.0 GPa [Fig. 6(b)] the Fermi level is empty and the system still has a gap of 0.19 eV. However, at $P=7.0$ GPa, we can observe in the DOS plot that the Fermi level is populated and the system is now metallic. Therefore, we can state that pressure induced a semiconductor-metallic transition between 6.0 and 7.0 GPa. Since the LDA calculations underestimate the gap, the real pressure where the semiconductor-metallic transition occurs should be somewhat larger than the value we have determined here. The states responsible for this metallic behavior [Figs. 6(c) and 6(d)] are two levels originally in the valence band (majority and minority spin) and one in the conduction band that cross each other in the Fermi energy along the R - X high-symmetry line. These levels near the Fermi energy primarily consist of Cu- $3d$ and O- $2p$ orbitals. The t_{2g} and e_g Ti- $3d$ levels are degenerate and upshifted by 0.5 eV compared with the uncompressed system. Thus, the pressure-induced electronic transition from semiconductor to metallic behavior in CCTO can be associated to the displacement of the Cu- $3d$ and O- $2p$ orbitals across the Fermi level. The electronic semiconductor-metallic transition is related to the relaxation of the atoms under applied pressure. The rearrangement of the system moves especially the O atoms from their original configuration, thereby generating different hybridizations with the other atoms. This is confirmed by analyzing the projected density of states (PDOS) of Cu- $3d$ and O- $2p$ orbitals shown in Fig. 7. The PDOS was calculated using the sum of majority and minority spin states. We can observe that for $P > 6.0$ GPa the Cu and O levels give a large contribution to the DOS at the Fermi level.

For uncompressed CCTO we estimate the magnetic moment of the CuO_4 complex to be $0.84\mu_B$. This cluster forms a spin-polarized unit with antiferromagnetic alignment of the magnetic moments on the Cu and O atoms. The Cu atom contributes $0.44\mu_B$ and each O atom contributes $0.10\mu_B$. For the system under pressure and also in the AF spin configuration, the magnetization of the CuO_4 is estimated as $0.35\mu_B$,

being $0.19\mu_B$ from the Cu atom and $0.04\mu_B$ from each O atom. These results show a decrease of the localized magnetic moment with increased pressure.

By using Mulliken population we estimate the ionic configuration for CCTO in the fundamental state to be $\text{Ca}^{+1.51}\text{Cu}^{+0.55}\text{O}^{-0.80}\text{Ti}^{+1.61}$. The (+) and (−) stand for loss and gain of charge. A large charge transfer between the atoms is observed. The Ca, Cu, and Ti atoms lose charge, transferring it to the O atoms. The ionic configuration for CCTO at 10.0 GPa is estimated to be $\text{Ca}^{+1.64}\text{Cu}^{+0.56}\text{O}^{-0.78}\text{Ti}^{+1.51}$. These results show that the Ca(Ti) atom decreases (increases) its total electronic charge when the applied pressure increases, while only small changes occur for the Cu and O atoms. This implies that the charge densities of Ca and Ti atoms are more sensitive to pressure variation than those of Cu and O atoms. We should point out that the numbers provide in the Mulliken analysis are strongly dependent on the basis set but the trends observed in the charge transfer process are reliable.

IV. CONCLUSIONS

We have studied the effects of pressure on the structural and electronic properties of antiferromagnetic $\text{CaCu}_3\text{Ti}_4\text{O}_{12}$ using *ab initio* total-energy calculations. Our results indicate

that at high pressures ($P > 3.0$ GPa) the more stable structure is rhombohedral, belonging to the $R\bar{3}$ space group rather than cubic ($Im\bar{3}$). Small tilting and deformation of the TiO_6 octahedra are the mechanisms responsible by the cubic-rhombohedral phase transition. The high-pressure electronic behavior is metallic rather than semiconductor with the transition occurring, according to our model, between 6.0 and 7.0 GPa. Therefore, we have predicted new physical phenomena to be observed in CCTO and this would stimulate experimentalists aiming to test the validity of the theoretical results. Furthermore, our results should be of interest in understanding the properties of CCTO thin films where stress plays a fundamental role.

ACKNOWLEDGEMENTS

The authors thank Professor R. B. Capaz for valuable discussions and suggestions. S.B.F. and A.G.S.F. acknowledge financial support from Universidade Federal do Ceará through visiting scientist grants and the CENAPAD-SP for the computer time. We thank Dr. A. Donegan for a critical reading of the manuscript. A.G.S.F. acknowledges the Brazilian Agency CNPq through Grant No. 307417/2004-2.

*Corresponding author, E-mail: solange@fisica.ufc.br

- ¹M. Subramanian, D. Li, B. Reisner, and A. Sleight, *J. Solid State Chem.* **151**, 323 (2000).
- ²A. P. Ramirez, M. A. Subramanian, M. Gardel, G. Blumberg, D. Li, T. Vogt, and S. M. Shapiro, *Solid State Commun.* **115**, 217 (2000).
- ³C. Homes, T. Vogt, S. Shapiro, S. Wakimoto, and A. Ramirez, *Science* **293**, 673 (2001).
- ⁴M. H. Cohen, J. B. Neaton, L. X. He, and D. Vanderbilt, *J. Appl. Phys.* **94**, 3299 (2003).
- ⁵D. Sinclair, T. B. Adans, F. Marrison, and A. West, *Appl. Phys. Lett.* **80**, 2153 (2002).
- ⁶L. He, J. Neaton, D. Vanderbilt, and M. H. Cohen, *Phys. Rev. B* **65**, 214112 (2002).
- ⁷L. He, J. Neaton, D. Vanderbilt, and M. Cohen, *Phys. Rev. B* **67**, 012103 (2003).
- ⁸N. Kolev, R. P. Bontchev, A. J. Jacobson, V. N. Popov, V. G. Hadjiev, A. P. Litvinchuk, and M. N. Iliev, *Phys. Rev. B* **66**, 132102 (2002).
- ⁹A. Koitzsch, G. Blumberg, A. Gozar, B. Dennis, A. P. Ramirez, S. Trebst, and S. Wakimoto, *Phys. Rev. B* **65**, 052406 (2002).
- ¹⁰Y. J. Kim, S. Wakimoto, S. M. Shapiro *et al.*, *Solid State Commun.* **121**, 625 (2002).
- ¹¹P. Hohenberg and W. Kohn, *Phys. Rev.* **136**, 864B (1964).
- ¹²W. Kohn and L. J. Sham, *Phys. Rev.* **140**, 1133A (1965).
- ¹³P. Ordejón, E. Artacho, and J. M. Soler, *Phys. Rev. B* **53**, R10441 (1996).

- ¹⁴D. Sánchez-Portal, E. Artacho, and J. M. Soler, *Int. J. Quantum Chem.* **65**, 453 (1997).
- ¹⁵O. F. Sankey and D. J. Niklewski, *Phys. Rev. B* **53**, R10441 (1989).
- ¹⁶The valence wave functions were described by a double-zeta polarized basis set of localized orbitals with cutoff radii for different atoms as follows: (i) oxygen: 3.93 a.u. for the $2s$ and 4.93 a.u. for $2p$ orbitals; (ii) copper: 7.82 a.u. for the $4s$ and 4.74 a.u. for the $3d$ orbitals; (iii) calcium: 9.52 a.u. for the $4s$ orbital; and (iv) titanium: 6.10 a.u. for the $4s$ and 5.95 a.u. for the $3d$ valence orbitals and for the semicore states 5.80 a.u. for the $3s$ and 5.80 for the $3p$ orbitals.
- ¹⁷J. P. Perdew and A. Zunger, *Phys. Rev. B* **23**, 5048 (1981).
- ¹⁸N. Troullier and J. L. Martins, *Phys. Rev. B* **43**, 1993 (1991).
- ¹⁹J. Junquera, M. Zimmer, P. Ordejón, and P. Ghosez, *Phys. Rev. B* **67**, 155327 (2003).
- ²⁰J. Junquera, O. Paz, D. Sanchez-Portal, and E. Artacho, *Phys. Rev. B* **64**, 235111 (2001).
- ²¹P. Ordejón, E. Artacho, R. Cachau, J. Gale, A. Garcia, J. Junquera, J. Kohanoff, M. Machado, D. Sanchez-Portal, J. M. Soler, and R. Weht, *Mater. Res. Soc. Symp. Proc.* **677**, AA.9.6.1 (2001).
- ²²A. L. Spek, *J. Appl. Crystallogr.* **36**, 7 (2003).
- ²³D. Valim, A. G. Souza Filho, P. T. C. Freire, S. B. Fagan, A. P. Ayala, J. M. Filho, A. F. L. Almeida, P. B. A. Fechine, A. S. B. Sombra, J. S. Olsen, and L. Gerward, *Phys. Rev. B* **70**, 132103 (2004).